ELSEVIER

Biochimica et Biophysica Acta 1370 (1998) 280–288

BIOCHIMICA ET BIOPHYSICA ACTA
BBA

Self-assembled α-hemolysin pores in an S-layer-supported lipid bilayer

Bernhard Schuster [a,*], Dietmar Pum [a], Orit Braha [b], Hagan Bayley [b], Uwe B. Sleytr [a]

[a] *Center for Ultrastructure Research and Ludwig-Boltzmann-Institute for Molecular Nanotechnology, Universität für Bodenkultur Wien, A-1180 Vienna, Austria*

[b] *Dept. of Medical Biochemistry and Genetics, Texas A&M Health Science Center, 440 Reynolds Medical Building, College Station, TX 77843-1114, USA*

Received 22 August 1997; revised 14 November 1997; accepted 20 November 1997

Abstract

The effects of a supporting proteinaceous surface-layer (S-layer) from *Bacillus coagulans* E38-66 on a 1,2-diphytanoyl-*sn*-glycero-3-phosphatidylcholine (DPhPC) bilayer were investigated. Comparative voltage clamp studies on plain and S-layer supported DPhPC bilayers revealed no significant difference in the capacitance. The conductance of the composite membrane decreased slightly upon recrystallization of the S-layer. Thus, the attached S-layer lattice did not interpenetrate or rupture the DPhPC bilayer. The self-assembly of a pore-forming protein into the S-layer supported lipid bilayer was examined. Staphylococcal α-hemolysin formed lytic pores when added to the lipid-exposed side. The assembly was slow compared to unsupported membranes, perhaps due to an altered fluidity of the lipid bilayer. No assembly could be detected upon adding α-hemolysin monomers to the S-layer-faced side of the composite membrane. Therefore, the intrinsic molecular sieving properties of the S-layer lattice do not allow passage of α-hemolysin monomers through the S-layer pores to the lipid bilayer. In comparison to plain lipid bilayers, the S-layer supported lipid membrane had a decreased tendency to rupture in the presence of α-hemolysin. © 1998 Elsevier Science B.V.

Keywords: Crystalline bacterial surface-layer (S-layer); Bilayer lipid membrane technique; Electron microscopy; Planar biomimetic membrane; Voltage clamp

1. Introduction

Crystalline bacterial cell surface layers (S-layers) represent the outermost cell envelope component in organisms of almost every taxonomic group of walled eubacteria and archaeobacteria (for compilations, see Refs. [1,2]). They are composed of a single protein or glycoprotein species with molecular weights ranging from 40,000 to 200,000 and can exhibit either oblique, square or hexagonal lattice symmetry [1,3,4].

The S-layer from *Bacillus coagulans* E38-66, used in the present study, represents a highly specialized supramolecular structure [5,6]. The characteristic features can be summarized as follows: (1) composition of identical, nonglycosylated protein subunits (M_r of 100,000); (2) oblique lattice symmetry with lattice

* Corresponding author. Center for Ultrastructure Research and Ludwig Boltzmann-Institute for Molecular Nanotechnology, Universität für Bodenkultur Wien, Gregor-Mendel-Straße 33, 1180 Wien, Austria. Fax: +43-1-4789112; E-mail: bschuste@edv1.boku.ac.at

PII S0005-2736(97)00274-5

constants of $a = 9.4$ nm, $b = 7.4$ nm, and base angle $\gamma = 80°$; (3) a thickness of about 5 nm; (4) anisotropic topographical surface properties; (5) very precise molecular sieving properties due to 3.5 nm diameter pores; (6) a charge neutral, more hydrophobic characteristic of the outer surface and a net negatively charged inner surface [5–7].

Isolated S-layer (glyco)protein subunits are endowed with the ability to assemble into monomolecular arrays at many different interfaces [3,7,8]. Previous studies have demonstrated that S-layer subunits from *B. coagulans* E38-66 recrystallize on lipid films generated by the Langmuir–Blodgett (LB) technique [7]. Transferred to solid supports, these composite lipid–S-layer structures were stable enough to allow lifting from the air–water interface and rinsing in water [9].

The aim of the present work was to study the influence of the attached S-layer on the integrity and electrophysical features of an artificial phospholipid bilayer, and to assemble a pore-forming protein within these lipid matrices. For this purpose, a folded phospholipid bilayer was formed over a thin Teflon aperture [10]. Subsequently, the S-layer protein was recrystallized on the lipid–water interface. Such composite S-layer supported lipid membranes mimic the cell envelope of those archaeobacteria that possess S-layers as the exclusive cell wall component external to the plasma membrane (for a review, see Refs. [1,11]).

In this study, the assembly and incorporation behaviour of the pore-forming protein α-hemolysin (αHL) was examined in plain and S-layer supported DPhPC bilayers. The exotoxin αHL is secreted from *Staphylococcus aureus* as a 293 amino acid [12], water-soluble monomeric polypeptide [13]. Seven copies of this monomer assemble to form heptameric pores [14] when presented with biological membranes [15], phospholipid vesicles [16]. A working scheme for the assembly of αHL pores has been devised. Water-soluble monomers bind to the lipid bilayer before associating to form a nonlytic heptameric 'prepore' [17,18]. Subsequently, the heptameric membrane-associated species inserts through the bilayer, forming a channel.

The recrystallization of the S-layer into large coherent areas and the assembly of proteinaceous αHL pores was monitored by electron microscopy. Voltage clamp measurements were performed to investigate the effect of the attached S-layer on the integrity and electrophysical features of the DPhPC bilayer. Furthermore, the formation of a DPhPC bilayer was proved by the assembly of αHL monomers to lytic pores, leading to an αHL-mediated increase in conductance. Isolated S-layer lattices showed precise molecular sieving properties [5] and revealed a stabilizing effect on solid supported lipid bilayers [9]. These features of the S-layer lattice can be employed for aperture-spanning lipid bilayers, especially when pore-forming proteins like staphylococcal αHL were assembled. The possibility of producing and making use of S-layer supported lipid bilayer as model target membranes for, e.g., engineered αHL pores [18,19] that can be modulated by nanomolar divalent metal ions will offer new applications as stable ion-selective biosensors.

2. Materials and methods

2.1. Isolation of S-layer subunits

Growth of *B. coagulans* E38-66 in continuous culture, cell wall preparations and extraction of S-layer protein with 5 M guanidine hydrochloride (GHCl) was performed as described previously [20]. GHCl extracts were dialyzed following this procedure, and the self-assembly products were sedimented for 15 min at $40{,}000 \times g$ at 4°C. The clear supernatant containing the disassembled S-layer subunits or oligomeric precursors (1.3 mg of protein per ml) was used for all recrystallization experiments.

2.2. Generation of the phospholipid monolayer

1,2-diphytanoyl-*sn*-glycero-3-phosphatidylcholine (DPhPC, Avanti Polar Lipids, # 850, 356) was dissolved in chloroform and stored at −20°C at a concentration of 12 mg lipid per ml solvent. For the generation of lipid monolayers, a homemade Langmuir–Blodgett (LB) trough with a surface area of 35 cm^2 and two barriers was used. The surface pressure was monitored with a homemade Wilhelmy plate apparatus. The LB-trough was filled with 20 ml standard buffer (2 mM $CaCl_2$, 10 mM KCl, adjusted with citric acid to pH 4.0; 22°C), a drop of the

DPhPC solution was spread on the air–water interface and compressed to a surface pressure of 25 to 28 mN/m.

2.3. Formation of the phospholipid bilayer

The 25-μm thick polytetrafluoroethylene film (Teflon, Goodfellow, Cambridge, England) apertures used in this study had a diameter of the orifice of 130 μm and were pretreated with a small drop of hexadecane/pentane 1:10 (Fluka, Buchs, Switzerland). The DPhPC solution (5 μl) was spread on the surface of each half-cell. One of the two half-cells (*cis* cell) was grounded, the other one (*trans* cell) was connected by an Ag/AgCl electrode to a voltage clamp setup (EPC 9, HEKA Elektronik, Lambrecht/Pfalz, Germany). Raising the level of the standard buffer within the two half-cells to above the aperture (final volume was 2.5 ml each) led to the formation of a folded DPhPC bilayer [10] that was checked by measuring the membrane conductance and capacitance.

2.4. Recrystallization of S-layer on DPhPC monolayer and on DPhPC bilayer

The recrystallization of S-layer subunits on DPhPC monolayers was performed as previously described for other phospholipids [7]. Briefly, after the generation of the DPhPC monolayer at the air–standard buffer interface, 2 ml of the supernatant of the S-layer solution were carefully injected into the standard buffer.

After forming the DPhPC bilayer, 0.4 ml of the supernatant of the S-layer solution was carefully injected into the *trans*-side of the lipid bilayer. Recrystallization of the S-layer subunits on the DPhPC–standard buffer interface was performed at 22°C overnight for all experiments.

2.5. Isolation and purification of α-hemolysin

The growth of *S. aureus* (FDA Wood strain 46, American Type Culture Collection) and the purification of αHL was performed as described previously [21]. The final concentration of the electrophoretically pure αHL-monomer stock solution was 0.8 mg protein per ml acetate buffer (10 mM Na-acetate, 20 mM NaCl, pH 5.0). In the monolayer experiments, 0.1 ml of the αHL stock solution was carefully injected into the subphase after generating the lipid monolayer. The final αHL–monomer concentration in the LB trough was 125 nM. In the bilayer experiments, 10 μl of the αHL stock solution were added either to the *cis* or to the *trans* side of the composite membrane. The final concentration of αHL monomers in one half-cell of the Teflon chamber was 100 nM for all experiments.

2.6. Electron microscopy

The recrystallization of the S-layer protein on the lipid–water interface, was examined by transmission electron microscopy (Philips CM12, Eindhoven, The Netherlands) of negatively stained preparations as described elsewhere [7]. In recrystallization experiments on DPhPC bilayers, the carbon-coated holey grids were pretreated with hexadecan/pentan (1:10) and placed on or near the thin Teflon film before DPhPC was spread. The composite S-layer-lipid film structure was generated on the holey grids in the same manner as described for bilayer formation across the Teflon septum.

2.7. Signal recording and data acquisition

The current response from given voltage functions were measured at 22°C to provide the electrophysical parameters of the plain and the S-layer supported DPhPC bilayers, and to study the assembly of the αHL pores. The data handling was performed on a Macintosh IIvx personal computer by the Pulse + PulseFit 7.4 software (HEKA Elektronik). Statistical analysis were performed using the Microcal ORIGIN program.

The settings of the two built-in Bessel filters of the EPC 9 amplifier for the current monitor signal were 10 kHz and 2.9 kHz. The current response to a rectangular voltage step (40 mV) was monitored to determine the conductance (G). A triangular voltage function (from +40 mV to −40 mV, 20 ms) was used to determine the capacitance (C) of the membrane. The calculated G and C values were divided by the area of the DPhPC membrane to give the specific conductance and capacitance, respectively.

3. Results

3.1. Recrystallization of S-layer protein on a DPhPC monolayer

To investigate the ability of the S-layer protein isolated from *B. coagulans* E38-66 to recrystallize on DPhPC films, monolayers were generated by the LB technique. As demonstrated by electron microscopical studies, S-layer subunits recrystallized into large coherent lattices also on the DPhPC monolayer (Fig. 1A). Such DPhPC monolayers, resembling one leaflet of a bilayer, were investigated as a matrix for the assembly of αHL heptameric pores. Indeed, electron microscopical studies clearly showed the formation of αHL oligomers (Fig. 1B).

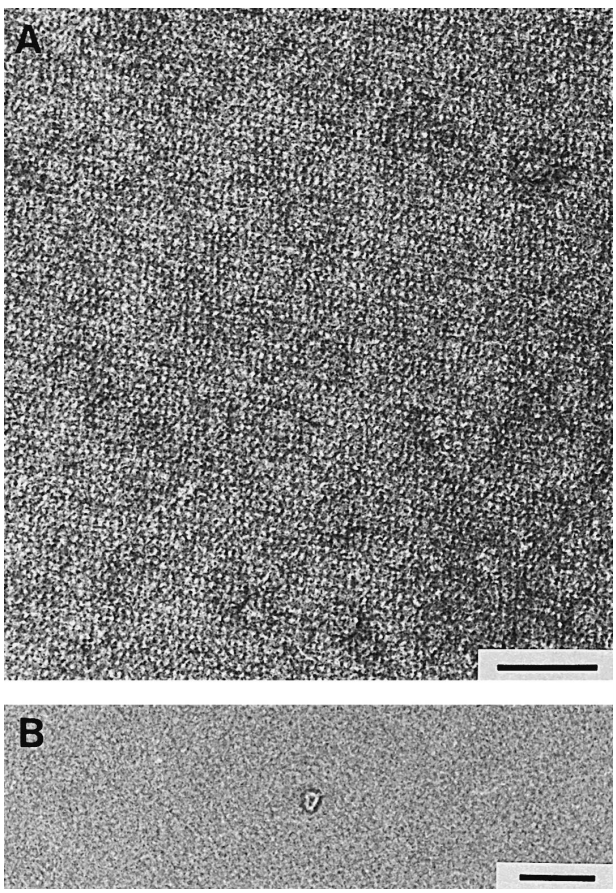

Fig. 1. Electron micrographs of (A) a coherent S-layer (*B. coagulans* E38-66) recrystallized on a diphytanoylphosphatidylcholine monolayer. The scale bar represents 0.1 μm. (B) Depicted is a diphytanoylphosphatidylcholine monolayer with an assembled α-hemolysin oligomer. The scale bar represents 50 nm.

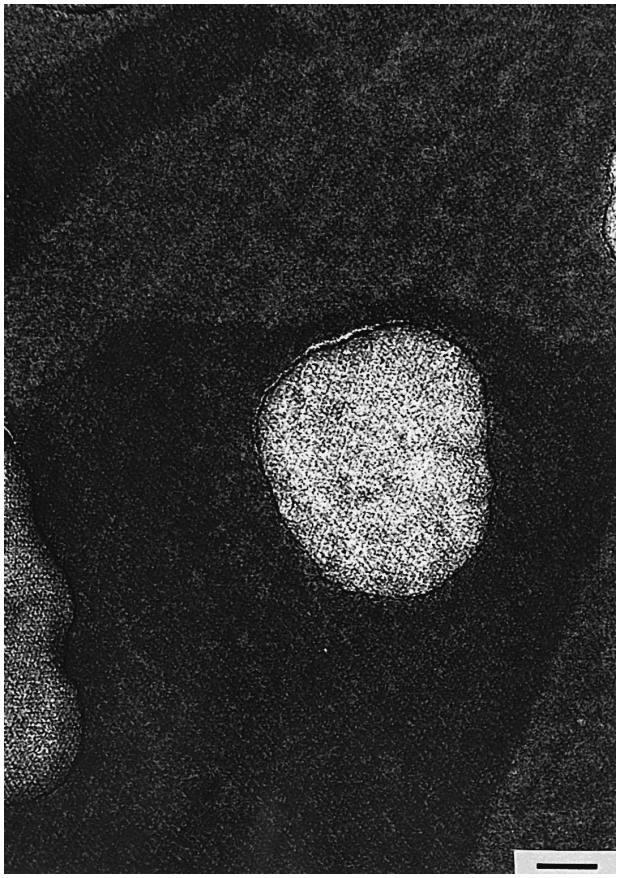

Fig. 2. Electron micrograph illustrating the crystallization of the S-layer protein of *B. coagulans* E38-66 on a diphytanoylphosphatidylcholine layer as described in the text. The scale bar represents 0.1 μm.

3.2. Recrystallization of S-layer protein on a DPhPC bilayer

S-layer protein was recrystallized on a DPhPC bilayer out of the standard buffer. Electron microscopy on holey grids showed coherent hole-spanning S-layer lattices (Fig. 2). Although the holey grids were placed on the Teflon film next to the aperture, in most cases one S-layer fully covered the holey grids, whereas a second S-layer recrystallized in large patches on the opposite side (Fig. 2). It was not possible to prove bilayer formation on the holey grids by electrophysical measurements as with the Teflon septum. However, these results clearly demonstrated the ability of the S-layer protein to recrystallize on DPhPC films under the chosen conditions.

Table 1
Electrophysical parameters of plain and S-layer-supported DPhPC bilayers

	G (pS)	G_s (μS/cm^2)	C_m (pF)	C_s (μF/cm^2)	t_d (nm)
Plain DPhPC bilayer	115.0 ± 51.8; $n = 9$	0.87 ± 0.04; $n = 9$	72.7 ± 6.1; $n = 9$	0.55 ± 0.05; $n = 9$	3.4 ± 0.3; $n = 9$
S-layer-supported DPhPC bilayer	72.3 ± 12.0; $n = 7$	0.54 ± 0.09; $n = 7$	74.7 ± 4.0; $n = 7$	0.56 ± 0.03; $n = 7$	3.3 ± 0.2; $n = 7$

G: membrane conductance.
G_s: specific conductance.
C_m: membrane capacitance.
C_s: specific membrane capacitance.
t_d: dielectric thickness of the hydrophobic core of the DPhPC bilayer.

3.3. Comparison of the electrophysical properties of plain and S-layer supported DPhPC bilayers

To determine the influence of an S-layer lattice attached to a phospholipid bilayer, the intrinsic electrical properties of plain and S-layer-supported lipid membranes were compared (Table 1). Most importantly, no disintegration of the lipid bilayer due to the recrystallization of the S-layer protein could be observed. On the contrary, the S-layer-supported phospholipid bilayer showed a lower conductance than the plain lipid bilayer. The capacitance and the dielectric thickness of the hydrophobic core, estimated from the measured capacitance (Table 1), were found to be in a good agreement with known data [22]. The capacitance of the S-layer supported DPhPC bilayer did not differ significantly compared with the unsupported lipid bilayer.

3.4. Assembly of αHL pores in plain and S-layer-supported DPhPC bilayers

The functionality of the αHL pore was investigated in plain and S-layer-supported DPhPC bilayers. As the DPhPC bilayer is symmetrical, αHL can be assembled into DPhPC bilayers either from the *cis* or from the *trans* side of the membrane. Upon αHL pore formation, the calculated conductance increased strongly and finally the bilayer ruptured after a time of ≤ 30 min ($n = 8$) (Fig. 3). A completely different behaviour was demonstrated for S-layer-supported DPhPC bilayers. αHL monomers added to the *trans*-side of the DPhPC bilayer, which was covered by the S-layer, produced no significant increase of the conductance as detected by voltage clamp measurements (Fig. 3). These results indicated that no assembly of the αHL monomers to form open pores had occurred (Fig. 3). The conductance measured over a long period of time did not vary significantly ($3.8\ \mu S/cm^2 \pm 1.2\ \mu S/cm^2$; $n = 4$) and the S-layer-supported DPhPC bilayer showed no tendency to rupture within at least 3 h. On the other hand, an increase in conductance could be observed when αHL monomers were added to the *cis* side of the S-layer supported DPhPC bilayer (Fig. 3), showing that assembly of functional αHL pores had occurred. Compared to plain lipid bilayers, the increase in conductance of the S-layer-supported lipid bilayer

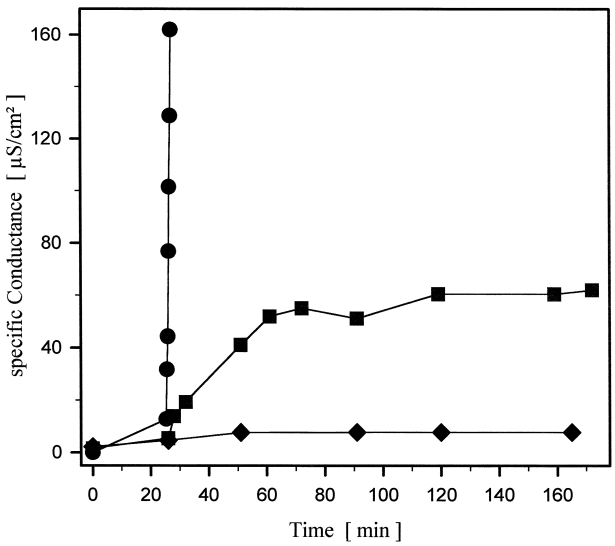

Fig. 3. A representative experimental run indicating the time-dependent conductance for a plain (●; *cis* side) and an S-layer-supported diphytanoylphosphatidylcholine bilayer after the addition of α-hemolysin (final concentration 1×10^{-7} M) to the *cis* (■) or to the *trans* side (♦) of the lipid membrane. The S-layer has previously been recrystallized on the *trans* side of the lipid bilayer. The conductance was calculated from the transmembrane current after a voltage step of 40 mV.

was not so pronounced (Fig. 3), and leveled off after 60 to 80 min to a conductance of 60.9 $\mu S/cm^2 \pm 9.0$ $\mu S/cm^2$ ($n = 4$). The integrity of this composite membrane, built of a phospholipid bilayer, an attached S-layer lattice and the transmembrane αHL pores was significantly enhanced (150 ± 22 min, $n = 4$) compared to the unsupported lipid bilayer (Fig. 3).

4. Discussion

In the present paper, we show that a tight biomimetic membrane, built up by a phospholipid bilayer and an attached crystalline proteinaceous S-layer, can be generated on an orifice with a diameter of 130 μm.

In order to investigate the ability of the S-layer protein isolated from *B. coagulans* E38-66 to recrystallize on DPhPC films and as quality control for determining the generation of a large, coherent S-layer lattice adjacent to the DPhPC film, LB experiments were performed. As demonstrated by electron microscopical studies, S-layer subunits recrystallized on the DPhPC monolayer (Fig. 1A) into large coherent lattices as previously observed with other lipid films [7,8]. Such DPhPC monolayers, resembling one leaflet of a bilayer system, were also most suitable for the screening of the best subphase conditions for both the S-layer recrystallization and the assembly of αHL monomers to heptameric pores. Indeed, electron microscopical studies clearly showed the formation of αHL oligomers (Fig. 1B). Since the functionality of the αHL pores assembled in the LB film could not be determined, it was not possible to distinguish whether the nonlytic 'prepore' [18] or the functional lytic pore had assembled on the DPhPC monolayer.

To investigate the influence of the S-layer on the DPhPC bilayer, the intrinsic electrical properties of plain and S-layer-supported membranes were compared. Since S-layer/DPhPC bilayers revealed a lower conductance than plain DPhPC bilayers (Table 1), it was obvious that upon recrystallization of the S-layer lattice, the integrity of the lipid membrane was not disturbed. Thus, in accordance with a previous study [23], noncovalent interactions between the S-layer subunits and the lipid film are not accompanied by an interpenetration of the lipid membrane by domains of the S-layer protein subunits.

The specific membrane capacitance and the dielectric thickness of the hydrophobic core of both membranes (Table 1) were in good agreement with known data [22]. Compared with the unsupported lipid bilayer, the capacitance of the S-layer-supported DPhPC bilayer did not differ significantly. The attached S-layer on the DPhPC bilayer was expected to produce a reduced capacitance due to the increased thickness of the composite lipid/protein membrane. However, the S-layer lattice is a highly porous structure with 3.5 nm pores [5], filled with water containing K^+ and Ca^{2+} ions. Furthermore, impedance measurements on artificial lipid bilayers revealed, in some cases, even a small increase in the measured capacitance as a result of the binding of streptavidin [24], although ellipsometry measurements clearly showed an increase in thickness of the membrane [24]. Since no increase in conductance could be observed upon adding αHL from the *trans* side (Fig. 3), it was concluded that under the experimental conditions, a coherent S-layer lattice had formed on the DPhPC bilayer. These results supported the electron microscopical examinations that always revealed an undisturbed complete S-layer.

As determined by voltage clamp experiments, the addition of αHL to both sides of plain DPhPC bilayers resulted in pore formation (Fig. 4A) as judged by the increase in conductance. A different behaviour was observed upon addition of αHL monomers to the *cis* or *trans* side of S-layer-supported lipid bilayers (Fig. 3). An increase in conductance that leveled off at 60.9 $\mu S/cm^2 \pm 9.0$ $\mu S/cm^2$ after a period of 60 to 80 min was measured when αHL monomers were added to the lipid-faced, *cis* side (Fig. 4B).

Recently, the crystal structure of the heptameric pore has been determined by X-ray crystallography to 1.9 Å resolution [25]. The structure resembles a mushroom, approximately 10 nm tall and up to 10 nm in diameter, with a pore running vertically through its centre. The mushroom stem constitutes the transmembrane domain and measures about 5.2 nm in height and 2.6 nm in diameter from C_α to C_α [25]. The length of the part of the β-barrel that sticks into the membrane is around 3 nm. The inner diameter of the pore is between 1.4 nm and 2.4 nm, and allows molecules of up to 3000 Da to pass through this water-filled channel [26,27]. Thus, in accordance with these structural data, the $\sim$3 nm transmembrane part

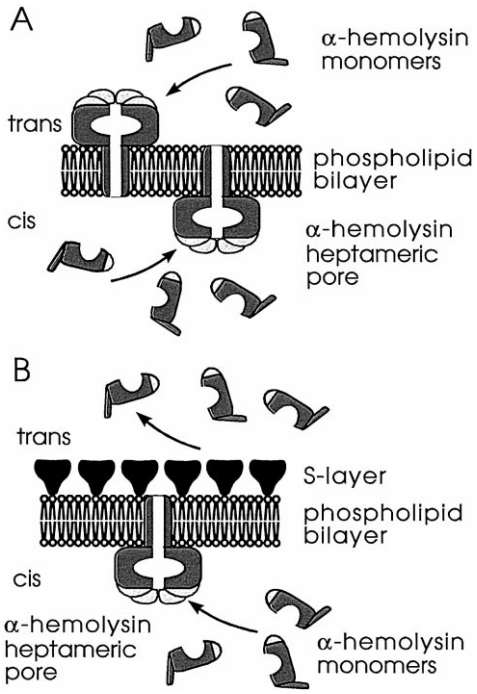

Fig. 4. Schematic illustration of the assembly of α-hemolysin oligomers in a plain (A) or in an S-layer-supported (B) diphytanoylphosphatidylcholine bilayer either from the *trans* or from the *cis* side of the membrane (not drawn to scale). Intermediate structures of the assembly process of α-hemolysin are not considered.

of the αHL heptamers had penetrated the hydrophobic region of the S-layer-supported DPhPC bilayer for which a thickness of approx. 3.3 nm was calculated (Fig. 4B, lower part).

The increase in conductance differed significantly between the plain and the S-layer-supported DPhPC bilayer. A recent study indicated that the recrystallization of an S-layer affects the order of the alkane chains of the lipid moiety by driving the fluid lipid into a phase of higher order [23]. According to the 'semifluid membrane' model [28], lipid head groups in the leaflet adjacent to the S-layer interact specifically with defined domains of the associated protein lattice, inducing an enhanced order, and reducing lateral diffusion within the lipid membrane [8,23,29]. The fluidity of lipid membranes is known to have an effect on the functionality of integral membrane proteins [30,31]. As mentioned above, it has been proposed that αHL monomers bind to membranes and heptamerization occurs upon their subsequent collision during lateral diffusion on the lipid bilayer [17,18,32]. In analogy to the effect of the S-layer recrystallization, a higher order of the lipid alkane chains is also induced by cooling down a phospholipid bilayer [33]. Previous studies demonstrated the ability of αHL to bind to cell membranes and to assemble to αHL oligomers at low temperatures, but the kinetics of both processes were slower [15,34]. The present result indicated that the more rigid lipid environment in an S-layer-supported lipid membrane might lower the binding efficiency of αHL monomers to the membrane and the subsequent assembly process to oligomers. Additionally, the final formation of a lytic pore might be hampered as the αHL domains forming the transmembrane part of the pore might penetrate the lipid layer associated with the S-layer lattice less easily. It can be expected that a considerable portion of the lipid molecules are restricted in their lateral mobility due to interactions with the S-layer protein. Furthermore, the αHL pores are only able to stick out of the DPhPC bilayer adjacent to the S-layer pores, but not at those areas where the S-layer subunits are attached to the head groups of the lipid film. In other words, it can be expected that the accessible lipid area for the formation of transmembrane, lytic αHL pores might be reduced compared to unsupported DPhPC bilayer. However, the time to measure S-layer-supported phospholipid bilayer with incorporated functional αHL pores was considerably improved under the same experimental conditions compared to unsupported DPhPC bilayer.

Voltage clamp measurements on lipid bilayers supported by a recrystallized S-layer on the *trans* side did not show a significant increase in conductance ($3.8\ \mu S/cm^2 \pm 1.2\ \mu S/cm^2$) upon adding αHL monomers to the *trans* side (Fig. 3). The coherent S-layer lattice apparently prevents access of αHL monomers to the lipid bilayer surface (Fig. 4B, upper part). Previous permeability studies on S-layer lattices from *B. coagulans* E38-66 showed free passage for myoglobulin ($M_r = 17{,}000$; molecular size 2.5 nm × 3.5 nm × 4.5 nm), but rejection of carbonic anhydrase ($M_r = 30{,}000$; molecular size of 4.1 nm × 4.1 nm × 4.7 nm) to 90% [5]. The crystal structure of the αHL monomer ($M_r = 33{,}200$) is not known, but a rough estimation of the molecular size might be derived from data of the heptameric pore [25] as the circular dichroism spectra of the αHL monomers and

heptamers are very similar [35]. This can only be an assumption of the shape of the αHL monomer, as structural changes upon formation of the heptamer can not be excluded particularly at the N-terminus and the central loop. However, from the crystal structure of the heptameric pore [25] it is known, that the rim domain of a single αHL monomer is shaped like an ellipsoid that measures 7 nm along the sevenfold axis, 4.5 nm wide and 2 nm thick [25]. Thus, it is unlikely that αHL monomers pass through the S-layer pores. Even if some αHL monomers did pass the S-layer and bind to the lipid bilayer, the S-layer lattice most likely would hinder the lateral diffusion of the αHL monomers, and thus the subsequent assembly to pores.

Recently, it was demonstrated that the small membrane-active molecule valinomycin could pass through the S-layer lattice and was incorporated into the lipid membrane [29]. In accordance with the data presented in this study, in S-layer-supported lipid membranes, the incorporation of valinomycin and the ion transport across the lipid layer was shown to be slower in comparison with unsupported lipid membranes.

Since S-layer-supported lipid membranes reveal a decreased tendency to rupture especially in the presence of ionophores [29] or pore-forming proteins, S-layer-supported lipid membranes represent an appealing biomimetic system for studying structural and functional properties of membrane proteins. In addition, light- [36] or ion-modulated [18] αHL mutant proteins assembled in S-layer-supported lipid membranes might become feasible leading to new nanotechnological applications particularly in sensor technology and electronic devices.

Acknowledgements

We thank Stefan Weigert for skilful technical assistance and Christopher Shustak and Stephen Cheley for purified α-hemolysin. This work was supported by grants from the Austrian Science Foundation, Projects S7204 (D.P.) and S7205 (U.B.S.), the Austrian Federal Ministry of Science, Transport and the Arts (U.B.S.), the Austrian National Bank, Project 5525, the US Army Research Office (H.B.) and the Office of Naval Research (H.B.).

References

[1] U.B. Sleytr, P. Messner, D. Pum, M. Sára, in: U.B. Sleytr, P. Messner, D. Pum, M. Sára (Eds.), Crystalline Bacterial Cell Surface Proteins, Academic Press, Austin, TX, 1996, pp. 1–34.
[2] P. Messner, U.B. Sleytr, in: A.H. Rose (Ed.), Advances in Microbial Physiology, Vol. 33, Academic Press, London, 1992, pp. 213–275.
[3] U.B. Sleytr, P. Messner, in: H. Plattner (Ed.), Electron Microscopy of Subcellular Dynamics, CRC Press, Boca Raton, FL, 1989, pp. 13–31.
[4] T.J. Beveridge, Curr. Opin. Struct. Biol. 4 (1994) 202–212.
[5] M. Sára, D. Pum, U.B. Sleytr, J. Bacteriol. 174 (1992) 3487–3493.
[6] M. Sára, U.B. Sleytr, J. Bacteriol. 175 (1993) 2248–2254.
[7] D. Pum, M. Weinhandel, C. Hödl, U.B. Sleytr, J. Bacteriol. 175 (1993) 2762–2766.
[8] D. Pum, U.B. Sleytr, in: U.B. Sleytr, P. Messner, D. Pum, M. Sára (Eds.), Crystalline Bacterial Cell Surface Protein, Academic Press, Austin, TX, 1996, pp. 175–209.
[9] B. Wetzer, D. Pum, U.B. Sleytr, J. Struct. Biol. 119 (1997) 123–128.
[10] M. Montal, P. Mueller, Proc. Natl. Acad. Sci. U.S.A. 69 (1972) 3561–3566.
[11] H. König, Can. J. Microbiol. 34 (1988) 395–406.
[12] G.S. Gray, M. Kehoe, Infect. Immun. 46 (1984) 615–618.
[13] S. Bhakdi, R. Füssle, J. Tranum-Jensen, Proc. Natl. Acad. Sci. U.S.A. 78 (1981) 5475–5479.
[14] J.E. Gouaux, O. Braha, M.R. Hobaugh, L. Song, S. Cheley, C. Shustak, H. Bayley, Proc. Natl. Acad. Sci. U.S.A. 91 (1994) 12828–12831.
[15] S. Bhakdi, J. Tranum-Jensen, Microbiol. Rev. 55 (1991) 733–751.
[16] H. Ikigai, T. Nakae, Biochem. Biophys. Res. Commun. 130 (1985) 175–181.
[17] B. Walker, M. Krishnasastry, L. Zorn, H. Bayley, J. Biol. Chem. 267 (1992) 21782–21786.
[18] B. Walker, O. Braha, S. Cheley, H. Bayley, Chem. Biol. 2 (1995) 99–105.
[19] O. Braha, B. Walker, S. Cheley, J. Kasianowicz, L. Song, J.E. Gouaux, H. Bayley, Chem. Biol. (1997) in press.
[20] U.B. Sleytr, M. Sára, Z. Küpcü, P. Messner, Arch. Microbiol. 146 (1986) 19–24.
[21] B. Walker, M. Krishnasastry, L. Zorn, J.J. Kasianowicz, H. Bayley, J. Biol. Chem. 267 (1992) 10902–10909.
[22] J. Stern, H.J. Freisleben, S. Janku, K. Ring, Biochim. Biophys. Acta 1128 (1992) 227–236.
[23] A. Diederich, C. Hödl, D. Pum, U.B. Sleytr, M. Lösche, Colloids Surf. B 6 (1996) 335–343.
[24] M. Stelzle, G. Weissmüller, E. Sackmann, J. Phys. Chem. 97 (1993) 2974–2981.
[25] L. Song, M.R. Hobaugh, C. Shustak, S. Cheley, H. Bayley, J.E. Gouaux, Science 274 (1996) 1859–1866.
[26] J.J. Kasianowicz, R.A. Brutyan, I. Vodyanoy, S.M. Bezrukov, Biophys. J. 66 (1994) A214.

[27] O.V. Krasilnikov, R.Z. Sabirov, V.I. Ternovsky, P.G. Merzliak, J.N. Muratkhodjaev, FEMS Microbiol. Immunol. 105 (1992) 93–100.
[28] U.B. Sleytr, M. Sára, P. Messner, D. Pum, J. Cell. Biochem. 56 (1994) 171–176.
[29] B. Schuster, D. Pum, U.B. Sleytr, Biochim. Biophys. Acta 1369 (1998) 51–60.
[30] E. Sackmann, in: R. Lipowsky, E. Sackmann (Eds.), Structure and Dynamics of Membrane, Elsevier, Amsterdam, 1995, pp. 213–304.
[31] G. Boheim, W. Hanke, H. Eibl, Proc. Natl. Acad. Sci. U.S.A. 77 (1980) 3403–3407.
[32] J. Reichwein, F. Hugo, M. Roth, A. Sinner, S. Bhakdi, Infect. Immun. 55 (1987) 2940–2944.
[33] P. Laggner, M. Kriechbaum, Chem. Phys. Lipids 75 (1991) 121–145.
[34] G. Belmonte, L. Cescatti, B. Ferrari, T. Nicolussi, M. Ropele, G. Menestrina, Eur. Biophys. J. 14 (1987) 349–358.
[35] N. Tobkes, B.A. Wallace, H. Bayley, Biochemistry 24 (1985) 1915–1920.
[36] C. Chang, B. Niblack, B. Walker, H. Bayley, Chem. Biol. 2 (1995) 391–400.